Relationship between Structures and Photocurrent Generation Properties in a Series of Hemicyanine Congeners

Ai-Dong Lang, Jin Zhai, Chun-Hui Huang,* Liang-Bing Gan, Yi-Lei Zhao, De-Jian Zhou, and Zhi-Da Chen

State Key Laboratory of Rare Earth Materials Chemistry and Applications, Peking University, Beijing 100871, People's Republic of China

*Received: July 25, 1997; In Final Form: October 24, 1997*

The relationship between structures and photocurrent generation properties in a series of dye congeners based on a hemicyanine template has been investigated by using their LB film modified ITO electrodes in a traditional three-electrode cell under the same conditions. Experimental data and semipirical quantum calculation results show that the molecular polarity is the key factor for the quantum yield of photocurrent generation in this kind of molecule. The effect of applied bias voltage, addition of electron donors and acceptors, and saturation degree of O_2 or N_2 on photocurrent generation of the selected one has also been examined.

Introduction

It is interesting to note that some organic dye molecules in which an electron donor and an electron acceptor group are linked together with a conjugation π-electron bridge not only exhibit high second-order hyperpolarizability coefficients but also show good photoelectric activities. This kind of molecular structure is easy to facilitate intramolecular electron-transfer reaction between donor and acceptor through the π-electron bridge with strong polarity effect[1,2] and may produce considerable photoelectric response signals. As examples of these attributes, several classes of organic dyes, such as merocyanine, azopyridinium, etc., whose second harmonic generation properties have been widely studied,[3−5] also have been extensively investigated for their photoelectrochemical behavior in LB films, and the quantum yields of these dyes are in the range of 0.01−0.1%.[6,7] These fundamental studies will be helpful for their potential usage in the areas of photoelectric conversion, photochemical switch, and information storage.

Hemicyanine dyes are a class of nonlinear optical materials well-known for their large second-order molecular hyperpolarizabilities coefficients.[8] Very recently, our group first reported the investigation of photoelectrochemical properties of a hemicyanine dye ((dimethylamino)stilbazolium chromophores) and its zinc complex LB film modified ITO electrodes, and the quantum yields are about 0.35% and 0.68%, respectively.[9,10] A possible mechanism for the photocurrent generation is also proposed. To design new molecules that have improved photocurrent generation properties, it is necessary to better understand the relationship between molecular structure and photoelectrochemical properties. In this paper, four hemicyanine analogues, (*E*)-octadecyl-4-[2-(4-dimethylaminophenyl)ethenyl]-pyridinium iodide (dye 1), (*E*)-octadecyl-4-[2-(4-diethylaminophenyl)ethenyl]pyridinium iodide (dye 2), (*E*)-octadecyl-4-[2-(4-dimethylaminophenyl)ethenyl]quinolinium iodide (dye 3), and (*E*)-[2-(4-dimethylaminonaphthyl)ethenyl pyridinium iodide (dye 4), have been selected, and photocurrent generations and quantum yields of their LB film modified ITO electrodes have been tested under identical conditions. The effect of molecular

CHART 1: Molecular Structure of the Four Hemicyanine Congeners
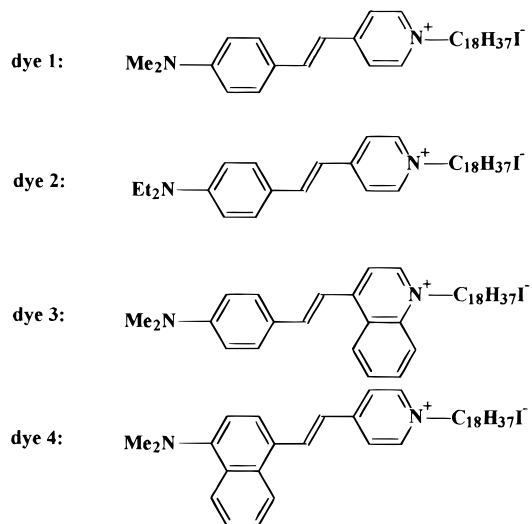
structure on photocurrent generation and quantum yield has been discussed according to the experimental data and semipirical quantum calculations. Additionally, one dye has been chosen to examine the effects of applied bias voltage, addition of electron donors and acceptors and saturation degree of O_2 and N_2 on photocurrent generation properties.

Experimental Section

1. Materials. The synthesis and characterization of the four hemicyanine dye congeners in Chart 1 have been reported elsewhere.[11,12] The hydroquinone (HQ) and ascorbic acid (AA) are all A.R. grade from Beijing Chemical Factory and are used as received. The methyl viologen diiodide (MV^{2+}) was synthesized by the reaction of 4,4 dipyridyl with excess methyl iodide in refluxing ethanol for 6 h. The product was filtered and then washed by ethanol four times, and its purity was characterized by the ^{1}H NMR. All the other chemicals are A.R. grade and are used as received. The water used as subphase is in-house deionized water purified by passing through an easy

---

Photocurrent Generation in Hemicyanine Dyes

J. Phys. Chem. B, Vol. 102, No. 8, 1998 **1425**

pure RF compact ultrapure water system (Barnstead Co.), and the resistivity is over 18 MΩ·cm.

2. π−A Isotherm and Film Deposition. LB films of each congener were prepared on a Langmiur−Blodgett trough (model 622, British NIMA Technology, Coventry) following the same procedure: chloroform solution of the dye was spread onto the deionized water subphase (13 ± 1 °C, pH = 5.6) and left 15 min for evaporation of chloroform, the floating film was compressed at the rate of 20 cm²/min, and the surface pressure area (π−A) isotherm was recorded. Substrates for LB films deposition in this paper were transparent indium−tin oxide (ITO) coated slides with 50 Ω lateral resistance. They were cleaned and pretreated hydrophilically following the traditional procedure[13] used before. For depositing a monolayer, an ITO slide was immersed into the subphase before spreading and the floating film was then compressed to an expected surface pressure such as 30 mN/m. After holding the surface pressure constant for 10 min, the monolayer film was deposited onto the slide with upstroking at a speed of 5 mm/min. The typical transfer ratios on substrates were about 1.0 ± 0.1.

3. Spectroscopic Measurement. The UV−vis spectra of the four dyes in solution or LB film were recorded on a Shimadazu UV-3100 spectrometer. Chloroform and a blank ITO slide were used as reference, respectively.

4. Photoelectrochemical Measurement. Photoelectrochemical experiments were carried out by using a conventional three-electrode setup. A LB film modified ITO slide was used as a working electrode (WE) with a 0.5 cm² effective contact area. The counter electrode (CE) was Pt foil, and the reference electrode was a saturated calomel electrode (SCE). KCl (0.5 mol L⁻¹) was used as supporting electrolyte for all the electronic measurements. The modified electrodes were irradiated with a 500 W xenon lamp (Ushio Electric). The photocurrent generation from the LB film modified electrode was detected by a voltammetric analyzer (model 600, CH Instrument). The action spectra were measured by the light from the Xe lamp passing through filters with a certain band-pass (Toshiba KL-40 ~ KL-80). The intensities of the incident beams were checked by a power and energy meter (model 372, Scientech) and then normalized in calculation. The IR light was filtered throughout the experiment with a Toshiba IRA-25S filter to protect electrodes from heating. All the measurements were carried out at the room temperature.

5. Semiempirical Quantum Calculation. In the present work, MINDO/3 in program system MOPAC 6.00 was used to calculate the net charge of atoms and dipole moment of the molecules. The molecular dynamic method was used to optimize the geometric structures of hemicyanine dye cations.

Results and Discussion

1. π−A Isotherm. π−A isotherms of the four hemicyanine dye congeners are shown in Figure 1, and some parameters obtained from Figure 1 are listed in Table 1. Data of the limiting area in Table 1, obtained by extrapolation of the solid-phase region of the isotherm to π = 0, are 0.95 and 0.96 nm² for dye 2 and dye 4, respectively; both of them are larger than that of 0.5 nm² for dye 1 and 0.60 nm² for dye 3. As the limiting area becomes larger, the collapse pressure drops from 44.0 mN/m for dye 1, 47.6 mN/m for dye 3 to 35 mN/m for both dye 2 and dye 4; meanwhile, the solid-phase slope decreases from 1.58 mN/m Å² for dye 1, 1.91 mN/m Å² for dye 3 to 0.65 and 0.75 mN/m Å² for dye 2 and dye 4, respectively. The possible reason for the differences of film formation properties of these four dyes lies in the fact that the balance between the hydrophobic
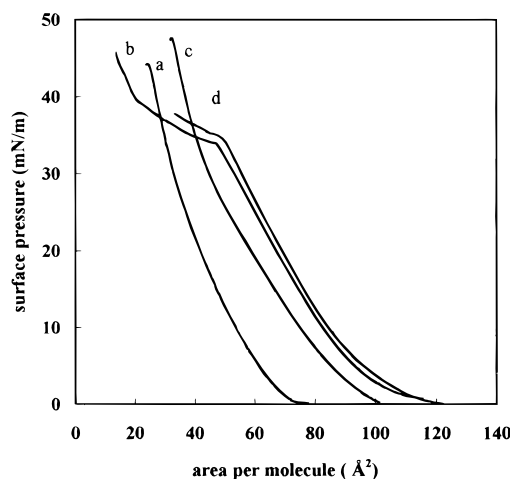
Figure 1. Surface pressure−area isotherm of the four hemicyanine dye monolayers at the air/water surface: dye 1 (a), dye 2 (b), dye 3 (c), dye 4 (d).

**TABLE 1: Parameters of the Monolayer Films of the Four Hemicyanine Dyes**

compd	limiting area (nm²)	collapse pressure (mN/m)	solide-phase slope (mN/mÅ²)
dye 1	0.50	44.0	1.58
dye 2	0.95	35.0	0.65
dye 3	0.60	47.6	1.91
dye 4	0.96	35.0	0.74

TABLE 2: UV−Vis Spectral Absorption Peaks of the Four Dyes

	absorption peak (nm)	
compd	in solution (CHCl₃)	in monolayer (ITO)
dye 1	503	490
dye 2	516	480
dye 3	561	560
dye 4	486	440

and hydrophilic parts of the molecule is very important to the film formation properties of hemicyanine dye molecules that have two alkyl chains on the nitrogen of the amino donor and a long octadecyl chain on the nitrogen of the pyridinium acceptor. Replacement of methyl on the nitrogen of the amino group in dye 1 by the ethyl in dye 2 or change of the benzene ring in dye 1 into a naphthalene ring in dye 4 makes both of the two terminals of the molecule take on some degree of hydrophobicity. As a result, molecules tend to stack loosely on the water surface with large tilt angles leading to larger limiting area and lower collapse pressure. On the other hand, the large improvement of the film formation properties of dye 3 is because the quinoline ring instead of pyridine ring enhances the hydrophobicity on one side of the molecule and makes the molecules arrange more perpendicularly on the water surface and stack closely resulting in a high collapse pressure.

2. Spectroscopic Characterization. Table 2 shows the absorption peaks of the UV−vis spectra in solution or mono-layers on the ITO glass of the four hemicyanine dyes. It can be observed from Figure 2 and Table 2 that all the absorption peaks of the four dyes in solution have characteristic π−π* electronic transition absorption bands around 500 nm due to their similar molecular structures. The slight change of the alkyl chain from methyl on the nitrogen donor in dye 1 to the ethyl in dye 2 leads to a 13 nm small red-shift from 503 nm for dye 1 to 516 nm for dye 2; this is attributed to that as a result of increasing the number of carbons *n*, the electron-donor character of a linear alkyl chain subtituent R=C*n*H₂*n*₊₁ increases.[14] The

1426 *J. Phys. Chem. B, Vol. 102, No. 8, 1998*

Lang et al.
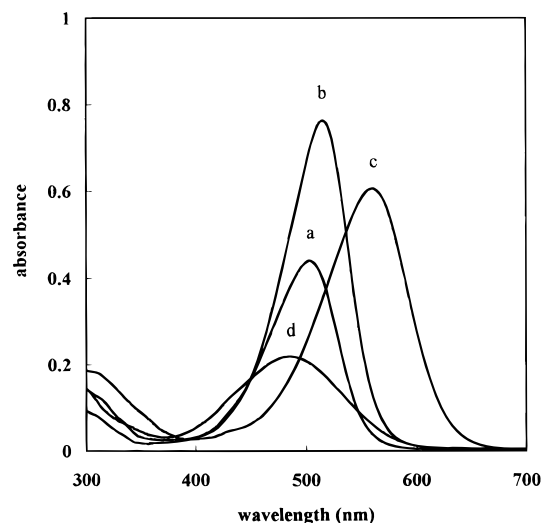
Figure 2. UV−vis absorption spectra of the four hemicyanine dyes in CHCl$_3$ solution: dye 1 (a), dye 2 (b), dye 3 (c), dye 4 (d).
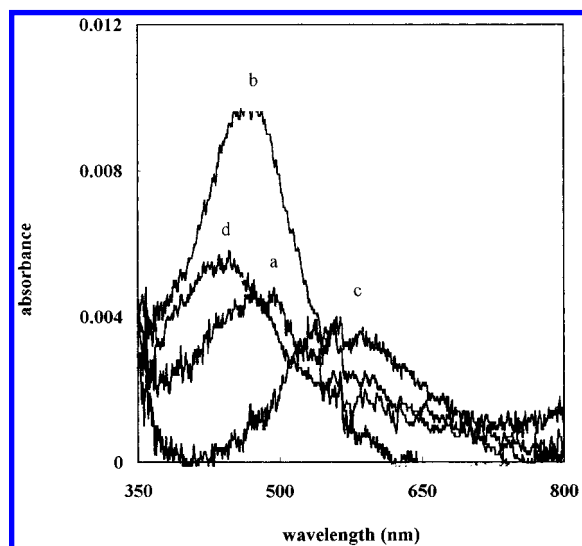

Figure 3. UV−vis absorption spectra of the monolayers of the four dye congeners on ITO slides: dye 1 (a), dye 2 (b), dye 3 (c), dye 4 (d).

replacement of the pyridium ring in dye 1 by the quinoline ring in dye 3 results in the large red-shift of 58 nm, since the quinolium ring is a more effective electron acceptor than the pyridium ring. On the contrary, replacing the phenyl ring in dye 1 by a naphthalene ring in dye 4 leads to a 19 nm blue-shift, indicating that although the naphthalene ring is a stronger π-electron conjugation system than the benzene ring, it is disadvantegous for the electron delocalization when the former is connected with the electron-donor group in the hemicyanine molecule.

Comparing the absorption peak in solution with that of corresponding monolayer film on an ITO slide (Figure 3), we can observe that a blue-shift occurs (13 nm for dye 1, 36 nm for dye 2, and 46 nm for dye 4), indicating that different degrees of H aggregates were formed in LB films of these dyes, whereas the absorption peak of dye 3 on ITO is very similar to that in solution, suggesting molecules exist as monomers in its LB film.

3. Photocurrent Generation Behavior from LB Film Modified Electrode. Steady cathodic photocurrents have been observed when each of the dye monolayer film modified ITO electrode is illuminated by a white light (86 mW/cm^2). The cathodic photocurrent−time plot of dye 3 (Figure 4) is given
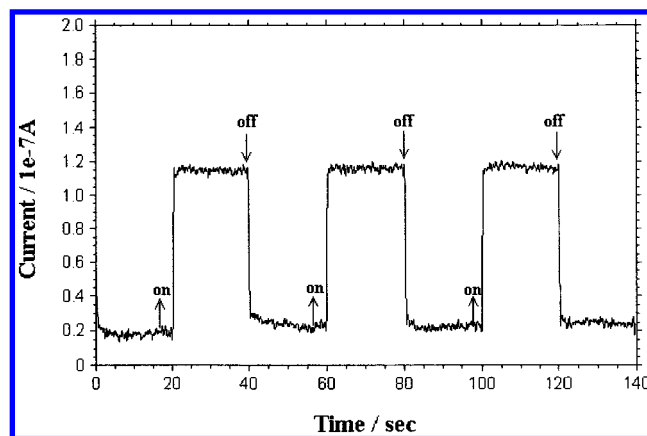
Figure 4. Photocurrent generation from dye 3 ITO electrode upon irradiation of white light at 86 mW/cm^2.
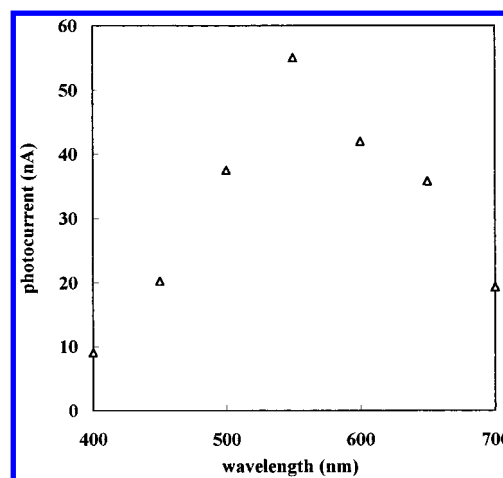
Figure 5. Action spectrum of dye 3 ITO electrode.

TABLE 3: Photocurrent Generation of Monolayer Film Modified ITO Electrode under Irradiation of Different Wavelengths

wavelength (nm)	photocurrent[a] (nA)			
	dye 1	dye 2	dye 3	dye 4
400	20.6	31.0	9.0	12.0
450	36.8	45.0	20.3	13.5
500	39.5	43.8	37.5	10.0
550	21.5	27.5	55.0	5.5
600	14.1	16.3	42.0	
650			35.8	
700			19.3	

[a] The intensities of different wavelengths were all normalized.

as an example. Generally speaking, the observation of cathodic photocurrent indicates that the electrons flow from the electrode through the LB film to the electrolyte solution. Figure 5 describes the action spectrum of the cathodic photocurrent generation of dye 3 measured under irradition of a white light (86 mW/cm^2) with filters, while Table 3 contains a list of action spectral data of other dyes. It can be found that all the spectral responses coincide very well with their absorption spectra of monolayers on ITO electrodes; the most effective wavelength is 450 nm for dyes 1, 2, and 4 and 550 nm for dye 3, suggesting that the hemicyanine dyes in LB films are responsible for the photocurrent generations.

To test the reproducbility of the photocurrent data, at least six ITO electrodes were fabricated and tested independently under the same conditions for each hemicyanine dye. Table 4 makes clear the values of photocurrent generated under the

Photocurrent Generation in Hemicyanine Dyes

J. Phys. Chem. B, Vol. 102, No. 8, 1998 **1427**

TABLE 4: Photocurrent and Quantum Yield of Dye Monolayer Film Modified Electrodes

compound	photocurrent[a] (nA)	quantum yield (%)[b]
dye 1	150−178	0.22
dye 2	201−244	0.14
dye 3	176−232	0.50
dye 4	50−78	0.087

[a] Irradited by white light of 86 mW/cm^2. [b] Irradited by white light of 86 mW/cm^2 through a band-pass filter: 450 nm for dye 1, dye 2, and dye 4; 550 nm for dye 3.
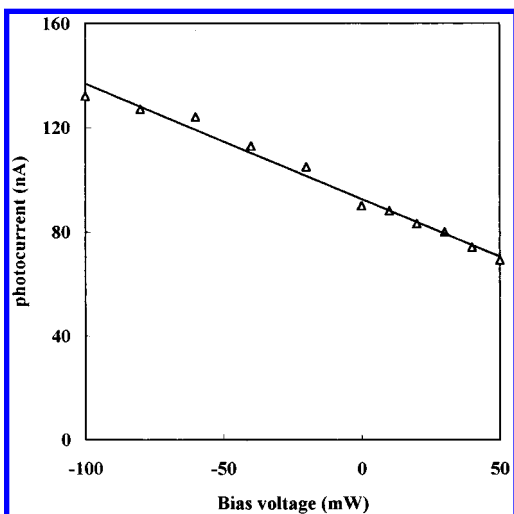
Figure 6. Effect of bias voltage on the photocurrent generation of dye 3 ITO electrode upon irradition of white light at 26 mW/cm^2.

Figure 7. Effect of MV^{2+} on the photocurrent generation from dye 3 ITO electrode in 0.5 mol L^{-1} KCl electrolyte solution upon irradition of white light at 26 mW/cm^2.

Figure 8. Effect of HQ on the photocurrent generation rom dye 3 ITO electrode in 0.5 mol L^{-1} KCl electrolyte solution upon irradition of white light at 26 mW/cm^2.

irradition of white light and the quantum yields generated under the maximal absorption wavelength. It is evident that the quantum yield of dye 3 is the largest among the four congeners.
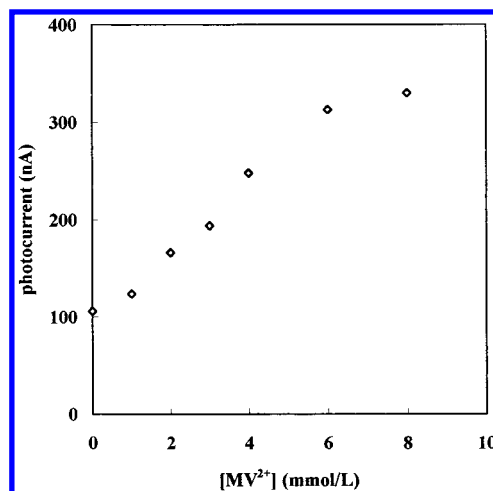
4. Effect of Some Factors on Photocurrent Generation of Dye 3−ITO Electrode. For the clearity of description, dye 3 is selected as a representative to discuss below, because it possesses the best film formation properties and the largest photocurrent among the four dyes.

Effect of Bias Voltage. There is a linear relationship between the observed photocurrent and the bias voltage (Figure 6) when the applied bias voltage is in the range of −100 to 50 mV (−SCE). The cathodic photocurrent increases with applied negative bias voltage added to the electrode, increasing from 0 to −100 mV and vice versa. The changing tendency is the same with other dyes congeners.

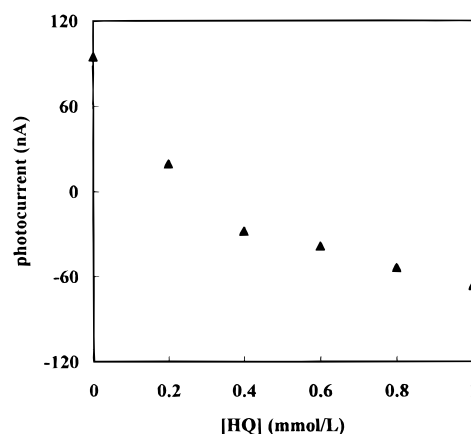*Effect of Electron Donors and Acceptors.* Several water-soluble electron donors and acceptors were added to the 0.5 mol L^{-1} KCl electrolyte solution to investigate their effects on photocurrent generation of the dye 3 monolayer film modified ITO electrode for furthur exploring the mechanism of photocurrent generation.

An increase of the photocurrent can be observed when the well-known electron acceptor methyl viologen (MV^{2+}) was added to the electrolyte solution as shown in Figure 7. The increase of the photocurrent slows down as the added MV^{2+} reaches 8 mmol L^{-1}. O$_2$ normally is treated as electron acceptor as it can accept an electron to form a superoxide anion. Saturation of the electrolyte with O$_2$ increases the photocurrent while degassing O$_2$ with N$_2$ decreases the photocurrent.

HQ is a relatively stronger electron donor, and a sharp decrease of the cathodic photocurrent can be produced when a very low concentration, 0.2 mmol L^{-1}, of it was added in the cell with dye 3 modified electrode as show in Figure 8. 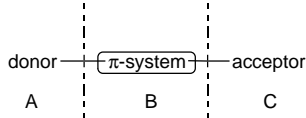The results show that HQ not only attenuates the anodic photocurrent but also redirects the flow of electrons to become an anodic photocurrent when the concentration is up to 0.4 mmol L^{-1} as in the squarine system.[15]

A small increase of the photocurrent can be observed by adding a weak electron donor AA. Although AA is an electron donor, it can still enhance the photocurrent rather than weaken the photocurrent. The electrolyte solution appears to be weakly acidic when AA was added into the 0.5 mol L^{-1} KCl electrolyte solution because AA is a weak acid. Here, the effect of pH value on the observed photocurrent may be more significant than the effect of donating an electron to the excited state.

5. Semiempirical Quantum Calculations. To better understand the ability of the photocurrent generation of these four hemicyanine derivative cations, their charge distributions and dipole moments both for the ground state and first single excited state have been calculated by using the MINDO/3 program. Limited by the cavity of the program, the model molecules used for calculation have carbon chains on the pyridinium rings shortened from 18 to 5 carbons to form dye 1′, dye 2′, dye 3′, and dye 4′ in comparison with our target molecules dye 1, dye 2, dye 3, and dye 4, respectively. Despite that, the results are valid for reference and comparison.

Charge Distribution. Table 5 summarizes the net charge in the ground and first singlet excited state of donor group (part A), π-system (part B), and acceptor group (part C). As can be seen from Table 5, the charge on part A in the ground state of

1428 *J. Phys. Chem. B, Vol. 102, No. 8, 1998*

Lang et al.

TABLE 5: Calculated Charge Distribution in the Ground and Excited State for Hemicyanine Dyes

donor —|— $\boxed{\pi\text{-system}}$ —|— acceptor

A · B · C

| compd	charge[a] in A[b]		charge[a] in B[b]		charge[a] in C[b]	
	ground state	excited state	ground state	excited state	ground state	excited state
dye 1′	0.0023	0.132	0.162	0.182	0.836	0.686
dye 2′	0.0046	0.160	0.153	0.185	0.842	0.655
dye 3′	0.0014	0.135	0.159	0.187	0.840	0.678
dye 4′	0.0361	−0.026	0.270	0.209	0.694	0.830

[a] The unit is the elementary electric charge (e).

TABLE 6: Calculated Dipole Moments in the Ground State and First Excited State (μ_g and μ_e) and the Difference between These Two States ($\Delta\mu_{eg}$)

compd	μ_g (D)	μ_e (D)	$\Delta\mu_{eg}$ (D)
dye 1′	9.64	5.07	−4.57
dye 2′	13.19	6.46	−6.73
dye 3′	6.95	2.57	−4.38
dye 4′	12.70	10.04	−2.66

dye 1′, dye 2′, or dye 3′ is all smaller than that for the excited state, while the charge on part C in the ground state is larger than that for the excited state, indicating that in the excited state of each of the three dyes, the electrons are donated to the acceptor group more than in the ground state; i.e, in the excited state, the electrons are easy to transfer from donor group through the π-electron conjugate system to acceptor group, and the charge separation occurs more easily. This result well explains the high ability of photocurrent generation of these three hemicyanine dyes. For dye 4′, we find just the opposite situation: the charge on part A in the ground state is larger than that in the excited state, while the charge on part C in the ground state is smaller than in the excited state, indicating that the electrons are donated from part A to pyridium ring in excited state less than in ground state. This may account for its relatively poor property in photocurrent generation. From Table 5, it also can be found that the change of charge in part C between the excited and ground state grows more obvious when the stronger donor or acceptor groups are attached to the molecule: the change of charge in part C is 0.1503e for dye 1′, 0.1874e for dye 2′ or 0.1613e for dye 3′. Data in Table 5 also show that ethyl is a stronger electron donor than methyl and that quinoline ring is a stronger electron acceptor than pyridium ring. These calculated results are in agreement with our experimental results that the quantum yields of dye 2 and dye 3 are larger than that of dye 1.

Dipole Moment. The calculated dipole moments in the ground state (μ_g) and the first excited state (μ_e) and the difference between μ_e and μ_g ($\Delta\mu_{eg}$) of the four dyes are listed in Table 6. For all the hemicyanine cations, $|\mu_g|$ are larger than $|\mu_e|$. This is in agreement with the stilbazolium derivitives.[16] We can also find that dye 4′ has the smallest $|\Delta\mu_{eg}|$ of 2.66 among the four dyes. Considering the calculation results of the electron distribution and the difference of the dipole moments, we can conclude that the structure of dye 4′ is not beneficial to the electrons separating and transferring from donor group to acceptor group in the excited state since the naphthalene ring in dye 4′ can block off the electrons transferring to the pyridium ring. These results support fairly our well experimental observations.
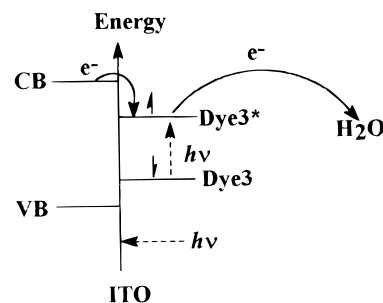
Figure 9. Proposed mechanism of the photocurrent generation of dye 3 ITO electrode.

6. Mechanism. We have proposed[9] that in a hemicyanine dye, the mechanism of the photocurrent generation is intramolecular electron-transfer reaction since in a hemicyanine dye molecule, a strong electron donor of dialkylamino and a strong electron acceptor of pyridium are linked together by a π-electron conjugation bridge. As shown in Figure 8, the cathodic photocurrent results from the excited state. The excited state accepts an electron from the conductive band of the ITO electrode and meanwhile transfers the electron to the electrolyte solution through the LB film; therefore, the polarity of the molecule and the difference of the energy levels of the HOMO and LUMO form important factors for photocurrent generation of the hemicyanine dyes (see Figure 9).

The data in Table 4 show that the photocurrents of dye 2 and dye 3 are higher than that of dye 1, while the photocurrent of dye 4 is lower than that of dye 1. Although the film formation properties can affect the photocurrent generation to some degree, the main factor is the polarity differences caused by molecular structure differerces among these four hemicyanine dyes. In their UV−vis absorption spectra, the red-shifts of the peak absoptions for dye 2 and dye 3 compared with that for dye 1 reveal the increase of the molecule dipole moment and the decrease of the difference of the energy level between the HOMO and LUMO in dye 2 and dye 4, which is beneficial to the electron separation and transfer in the molecule. The blue-shift of the peak absorption of dye 4 means the decrease of the molecule dipole moment and the increase of the difference of the energy level between the HOMO and LUMO, which are disadvantageous for the electron separation and transfer in the molecule. These results suggest the fact that using a more effective donor group or a more effective acceptor group would be helpful to enlarge molecule polarity in hemicyanine dyes and to get a large photocurrent.

As we know that calculation of the quantum yield should take into account the absoption ratio of the monolayer on ITO glass, this explains why the quantum yield of dye 2 is smaller than that of dye 1, attributed to its larger absorption ratio (1% for dye 1 and 2% for dye 2).

Conclusion

Photocurrents and quantum yields of the four hemicyanine dye analogues have been measured under the identical conditions. The experimental results show that dye 3 with a stronger electron acceptor group exhibits excellent photoelectrochemical behavior and its quantum yield is 0.5% under ambient conditions. Dye 2 with a relatively more effective electron donor group has relatively larger photocurrent than dye 1. The relationship between molecular structure and photocurrent generation has been explained according to the UV−vis spectral data and semiempirical calculation results. We believe the results can shed light on designs of new photoelectroactive

Photocurrent Generation in Hemicyanine Dyes

J. Phys. Chem. B, Vol. 102, No. 8, 1998 **1429**

molecules. The effects of applied bias voltage and the added electron donor and acceptor on photocurrent generation of dye 3 suggest that the mechanism of photocurrent generation proposed to dye 1 is also suitable to dye 3.

References and Notes

(1) Huang, C. H.; Zhao, C. H.; Zhuo, Y. F. *Langmiur* **1994**, *10*, 3794.

(2) Matsuo, T.; Itoh, K.; Takuma, K. *Chem. Lett.* **1980**, 1009.

(3) Dulcic, A. *Chem. Phys.* **1979**, *37*, 57.

(4) Girling, I. R.; Kolinsky, P. V.; Montgomery, C. M. *Electron Lett.* **1985**, *21*, 169.

(5) Li, H.; Huang, C. H.; Zhao, X. S. *Langmiur* **1994**, *10*, 3794.

(6) Saite, K.; Yokoyama, H. *Thin Solid Films* **1994**, *234*, 526.

(7) Xia, W. S.; Huang, C. H.; Luo, C. P. *J. Phys. Chem.* **1996**, *100*, 15525.

(8) Ashwell, G. J.; Hargreaves, R. C.; Balduwin, C. E. *Nature* **1992**, *357*, 393.

(9) Xia, W. S.; Huang, C. H.; Gan, L. B.; Li, H. *J. Chem. Soc., Faraday Trans.* **1996**, *92* (17), 3131.

(10) Xia, W. S.; Huang, C. H.; Zhou, D. J. *Langmiur* **1997**, *13*, 80.

(11) Li, H.; Zhou, D. J.; Huang, C. H. *J. Chem. Soc., Faraday Trans.* **1996**, *92* (4), 2585.

(12) Li, B. F.; Jiang, L. *J. Chin. Chem. Phys.* **1993**, *6* (2), 134.

(13) Zhou, D. J.; Huang, C. H.; Li, H. *Solid State Commun.* **1996**, *99* (10), 739.

(14) Ulman, Abraham. *Ultrathin Organic Film*; Academic: New York 1991; pp 352−356.

(15) Kim, Y. S.; Liang, K. N.; Law, K. T. *J. Phys. Chem.* **1994**, *98*, 984.

(16) Duan, X.-M.; Konami, H.; Okada, K.; Oikawa, H.; Matsuda, H.; Nakanishi, H. *J. Phys. Chem.* **1996**, *100*, 17780.